International Journal of Research in Advanced Engineering and Technology
ISSN: 2455-0876; Impact Factor: RJIF 5.44
www.engineeringresearchjournal.com
Volume 3; Issue 1; January 2017; Page No. 32-40

Fixed bed adsorption study for removing of reactive orange 16 and acid red 114 dyes from aqueous solution using Kenaf

[1] Maytham Kadhim Obaid, [2] Luqman Chuah Abdullah, [3] Dalia Sadiq Mahdi, [4] Intidhar Jabir Idan, [5] Siti Nurul Ain Binti Md. Jamil

[1, 2, 4] Department of Chemical and Environmental Engineering, Faculty of Engineering, Universiti Putra Malaysia
[1, 4] Department of Environmental Engineering, Faculty of Engineering, University of Babylon, Hilla, Babylon, Ira
[5] Faculty of Science, Universiti Putra Malaysia, 43400 Sardang, Salengor, Malaysia
[3] Faculty of Biotechnology, University of Al- Qasim Green Babylon, Iraq

Abstract
Kenaf fiber has proved its ability to remove dyes from aqueous solutions. This natural material is characterized by its abundant, relatively low cost and eco-friendly. In this study, kenaf core fiber was modified by adding trimethyl-chloro-bilateral-hydroxypropyl trimethyl ammonium chloride as a quaternizing agent to the constituent in order to increase its ability to adsorb dyes more efficiently. In fixed bed column model, Adsorption experiment was carried out to investigate the effect of height, initial dye concentration, flow rate, and regeneration. Maximum bed capacity, percentage dye removal and equilibrium dye uptake were determined and breakthrough curves were plotted. It was observed that adsorption was higher at lower flow rate, higher bed depth and lower initial dye concentration for two dyes. Maximum bed capacity of 3.25 g was obtained at a flow rate of 10 ml/min, bed height of 7.5 cm and initial dye concentration of 100 ppm. Data from column studies were fitted to three well established column models, Thomas model, Adams-Bohart model and Yoon-Nelson model. The experimental data were in good agreement with theoretical results. The study revealed the applicability of kenaf in fixed bed column for removal of dyes.

Keywords: acid red114, reactive orange16, modified kenaf center fiber, adsorption

1. Introduction

For decades, the environment suffers from pollution problems, especially the aquatic environment. The water is one of the main reasons for creations presence on the ground. The history of previous civilizations indicated that these communities preferred living close to water sources. Therefore, our existence with healthy life is highly related with fresh and clean water [1]. Water enters in many industrial aspects such as textile, tanning, plastic, printing, carpet and many other industries [2]. These industries need a large amount of water in various subsequent operations [3]. The contaminant water was usually discharged into rivers without serious care especially in developing countries that lacking of strict laws regarding environment protection. Sometimes, the concentration of dyes might reach a high level of about 15% [4]. Nitrogen colors (AZO) make up 60% of the colors found in food [5]; therefore, directly or indirectly could reach rivers, streams, ponds, water bodies [6]. Subsequently, the pollution of water has been started [7]. This pollutant could be found mostly in the effluent in many sewage treatment plants. Large quantities of these dyes were disposed to the environment, especially in the streams and rivers [8]. The interest in environmental affairs has been increased to treat the disposed water from textile factories [9]. 20% of the water pollution caused by the textile industry on the level the globe [10]. This large amount of pollutant dyes has become a source of concern [11]. Moreover, it might impact the aesthetic nature of water and aquatic life. Some dyes have complex structures and they possess high resistance to hydrolysis. This could prevent the sun's rays, increase oxidation and toxicity, kill aquatic life, mutagenic and cause cancer. Eventually, this contaminated water has been accumulated in the soil. Consequently, a lot of researchers have interested to remove these dyes before putting them away in rivers. Adsorption characterised by its simplicity, ease of using and desired outcomes without harmful substances. Therefore, adsorption might be the best and most suitable method in comparison with traditional methods such as chemical, physical, biological and other common methods [12]. Most of these methods were impractical, expensive, and difficult in implementation and low efficiency. Recently, researchers came to find alternative materials characterised by their availability and relative cheapness such as the ones that come from agricultural crops (see Table 1). In this research, the modified kenaf core fibre (MKCF), shown in Figures1 (a and b) natural kenaf. Kenaf plant is an agricultural crop which is widely available in several countries. In Malaysia, Kenaf plant has been ranked as the nation's seventh commodity [23]. Acid dye utilised in many products such as nylon, wool, silk, paper, leather, printing and canned food.

Table 1: Agricultural waste used in previous studies as an absorbent.

Dyes	Adsorbents	q_{max} (mg/g)	Ref.
Methylene blue	Modified Durian Leaf Powder	125	[2]
Reactive Blue19	Wheat Straw	4.22	[13]
Reactive Yellow 2(RY2)	Cocoa (Theobroma Cacao) Shell	333.33	[14]
Phenol	carbonized coir pith	48.31	[15]
Red denoted as RR	Green Carbon	28.25	[16]
brilliant blue reactive (RBBR)	pomegranate peel activated carbon	370.86	[17]
Reactive orange	hyacinh root powder	17.24	[18]
Methylene blue	corn cob powder calcined	41.33	[19]
Methyl Red	Montmorillonite	84.28	[20]
mercury ion	fir wood sawdust	129	[9]
lead(II)	rubber leaf powder (CARL)	97.19	[21]
Reactive red 228	Quaternized Flax shive	190.0	[22]
Acid red 114	Modified kenaf core fibers	232.56	This work

Fig 1(a): Kenaf plant

Fig 1(b): Cross-section of Kenaf stem

Materials and Methods

Preparation of Modified Kenaf Core Fibers (MKCF)

The kenaf fibers (core chips) placed inside the dryer for an hour at 50^0C to make sure to get rid of moisture. Second, the dried materials were grinded and have been sieved to get a fiber with size ranged between 0.25 to 1 mm. The granular Kenaf center fibers (KCF) was subsequently washed by using distilled water and then dried at same previous temperature, Show figure 2 (a and b).

Fig 2(a): Kenaf before treatment

Fig 2(b): Kenaf after treatment

The modification in Kenaf fibers includes surfaces treatment to increase its adsorption ability. This modification could increase the number of pores on the kenaf surface. In order to modify the Kenaf fibers, three major steps have been employed. These main steps included mercerization, quaternization and rinsing and drying. The mercerization step, each 60 gram of dried Kenaf fibers were drenched in 125 gram of NaOH mixed with 500mL of water during 20 hour in a glass pot. This step was very important for expanding the existed pores and adapting them to adsorb more dyes. Mercerized kenaf fibers were washed and placed in the oven at a temperature of 50 ^{o}C. Dried mercerized Kenaf fibers were then weighed again to prepare them for the next step. In step two, the quaternization process, each two grams of KCF

added to 3: 8: 5 w/w proportions from NaOH, trimonthly-chloro-bilateral-hydroxypropyl trimethylammonium chloride and water respectively. The resulted mixture was then wetted by distilled water and covering it by aluminum foil for 24 hour at ambient temperature. Before rinsing and drying the modified Kenaf fibers, distilled water with 0.3% HCL acid added to the water in order to prevent the response for one hour. Lastly, the product was rinsing by distilled water up to getting pH (7-8) and then dried at 50 ^{o}C.

Preparation stock solution dye

The solution dye was prepared by dissolving (1 gram) of orange16 (OR16) and acid red 114 (AR114) in (1 L) of distilled water and mixed well. The mixture was then kept inside a container for 24 hour in a dark place to ensure it would be homogenous and firmly spread. Properties of OR16 and AR114 dyes are listed in Table 2 and the compound structure. The wavelength mixture was checked using a spectrophotometer UV-1800 (SHMADZU) and compared with that provided by the supplier. The result was conformed to the provided data. All UV tests were achieved using filter paper to isolate the Kenaf from the aqueous solution. In figure (3) the Chemical structure of reactive orange16 and acid red114.

Table 2: General properties of reactive orange 16 and acid red 114

Property	Description	
Name of the commercial dye	Acid red 114	Reactive orange 16
Molecular weight (g/mol)	830.81	617.54
λ max (nm)	518 nm	493 nm
Chemical formula	C37H28N4Na2O10S3	C20H17N3Na2O11S3
Physical state	Dry powder	Dry powder
Dye content	45 %	≥70 %

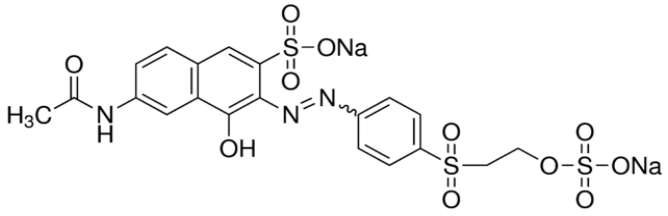

(a)

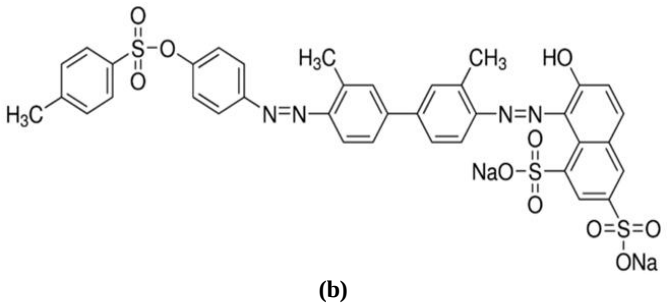

(b)

Fig 3: Molecular structure of adsorbate: (a) RO16; (b) AR114.

Result and discussion

Morphological characterization (SEM)

The morphological features and physical surface characteristics of natural kenaf core fibres (NKCF) and modified kenaf core fibres (MKCF) were analyzed by using Scanning Electron Microscope (SEM). The SEM images are shown in Figure 4 (a), (b), (c), and (d) for natural KCF, mercerized KCF, modified KCF and modified KCF after adsorption dye, respectively. As shown in Figure 4 (a), it can be clearly seen that the surface of raw kenaf particles was appeared fibrous, smooth, and constituted by sheaves of narrower fibres surrounded by a lingo-cellulosic cover. Mercerised kenaf core fibres Figure 4 (b) appeared as highly heterogeneous pores of honeycomb shape structures. As shown in Figure 4 (c), the modified process form a rough surface and exhibit different cylindrical channels. The presence of these open cylindrical and heterogeneous pores provides good sites for dyes to be trapped and adsorbed on MKCF surface [24]. Figure 4 (d) shows clearly the dye-loaded adsorbent coated by dye molecules over the whole surface.

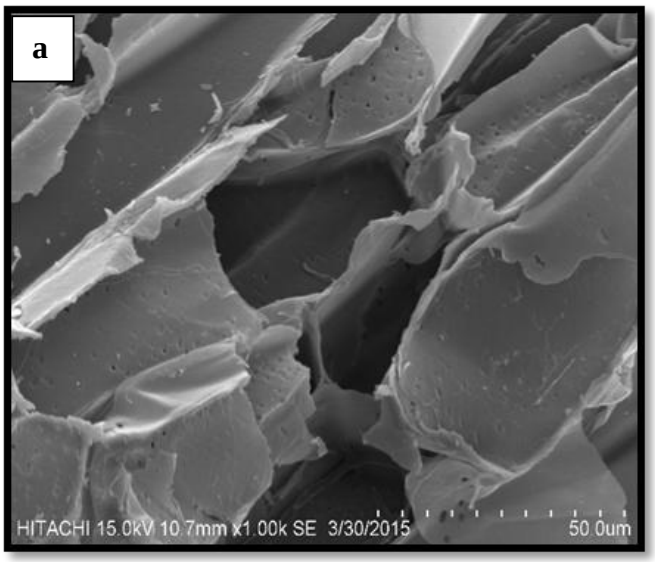

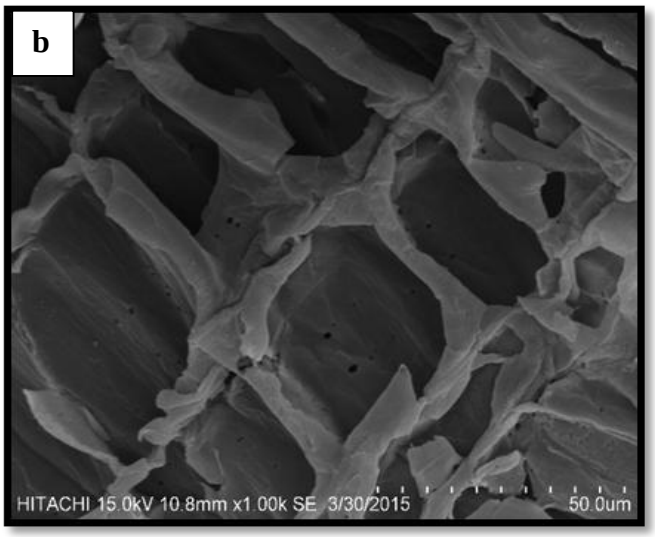

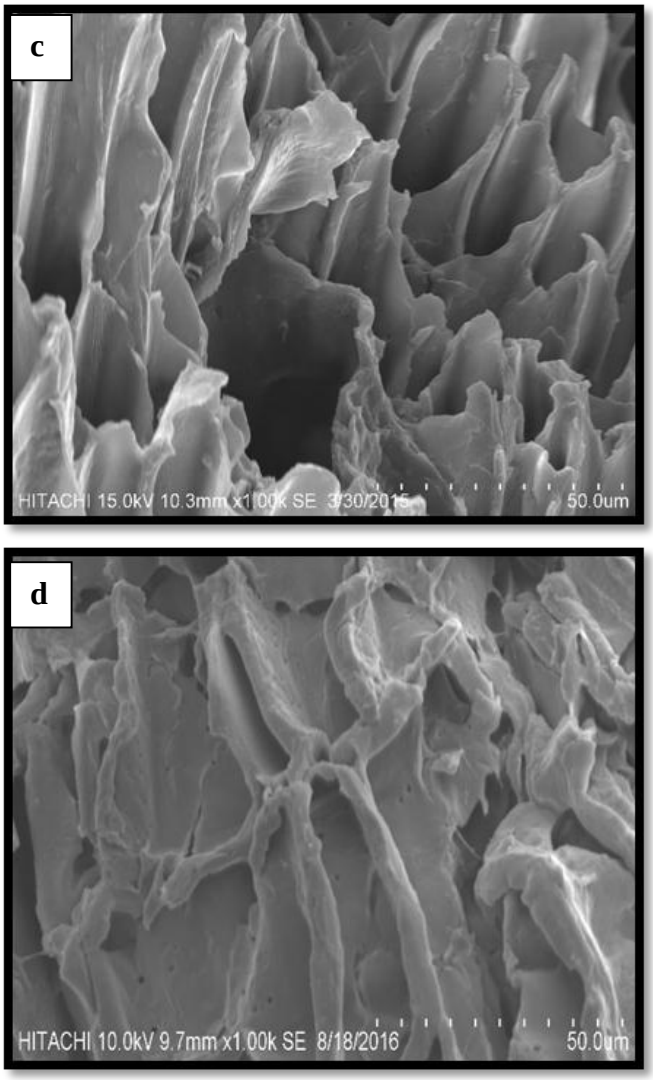

Fig 4: SEM micrograph for (a) NKCF (b) Mercerised KCF (c) MKCF and (d) MKCF after dyes adsorption.

Fourier Transform Infrared (FTIR) Spectroscopy

The FTIR spectrum is a primary tool to identify the characteristic functional groups which can contribute to enhance adsorption efficiency of the MKCF for adsorption dyes. The major and minor peaks recorded for natural kenaf core fibres (NKCF) and modified kenaf core fibres (MKCF) are showed in Figure 5, and listed in Table 3.

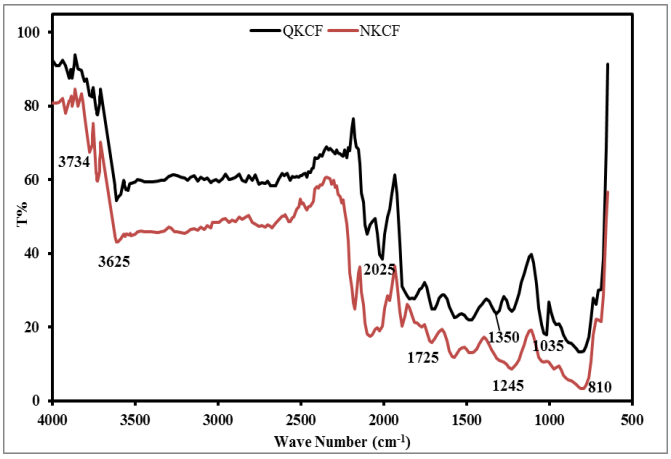

Fig 5: FTIR spectra for NKCF and MKCF

Table 3: Analysis of FTIR spectra of NKCF and MKCF

Frequency for NKCF (cm^{-1})	Frequency for MKCF (cm^{-1})	Assignment
3734	3734	O-H stretching
3625	3625	O-H stretching
-	2025	C-H stretching
1725	1725	C = O stretching
-	1350	O-H bending
1245	1245	C-O stretching
-	1035	C-O-C stretching
810	810	CH_2 rocking

BET Analysis

The BET analysis of MKCF and NKCF has revealed that the surface area (SBET) increased from 2.3 m^2/g for NKCF to 4 m^2/g for MKCF and the average pore diameter increased from 105.5 nm for NKCF to 283 nm for MKCF. Enlargement of the pore size is due to the dissolved lignin and hemicellulose in NaOH solution during the mercerization process. Hence, increase the surface area of cellulose that can react to quaternizing agent. Furthermore, pore volume slightly decreased from 0.1699cm^3/g for NKCF to 0.1128 cm^3/g for QKCF. It is attributed to the smoother texture of KCF surface after chemical quaternization.

Particle size distribution

Particle sizes for MKCF with a log-normal distribution are shown Figure 6. The most widely used method of describing particle size distributions are D values. The D10, D50 and D90 are commonly used to represent the midpoint and range of the particle sizes of a given sample. From the results of Particle size distribution, the D10, D50 and D90 were 15.391, 71.342 and 502.201µm respectively. Particle sizes distribution is a very important parameter to be considered when selecting suitable adsorbent particle size. Smaller particle size yields better removal efficiency because smaller particle sizes have larger surface area and that will increase the number of active sites for adsorption, however, fine particles that have difficult and long settling time are not favored as they will cause a problem in separation after the adsorption process. Therefore, the adsorbent particle size must be choosen according to their removal efficiency, settling time, and cost factor.

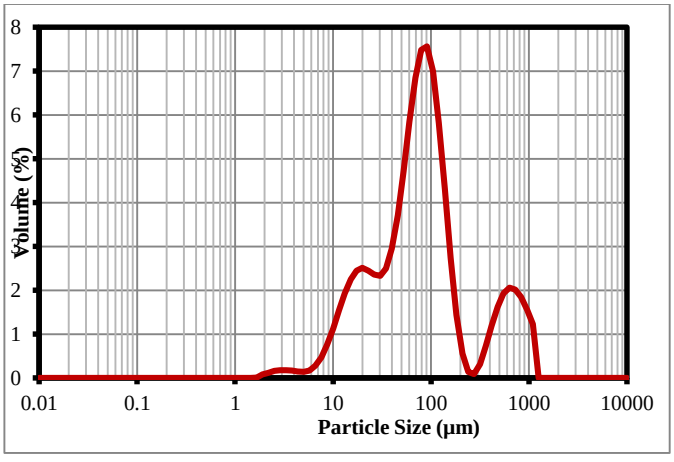

Fig 6: Particle Size Distribution for MKCF.

Effect of flow rate on breakthrough curve

By varying the inlet flow rate of dye from 10 ml/min to 14 ml/min, the following trend was observed on break through curve. Figures (7 and 8) and show that faster break through occurred at higher flow rate for both dyes. At lower flow rate, there was adequate time for the dye solution to be in contact with adsorbent, which resulted in a greater removal of RO16 and AR114 molecules in column. Higher dye removal occurred at lower flow rates for both dyes. The break through curve became steeper at higher flow rate.

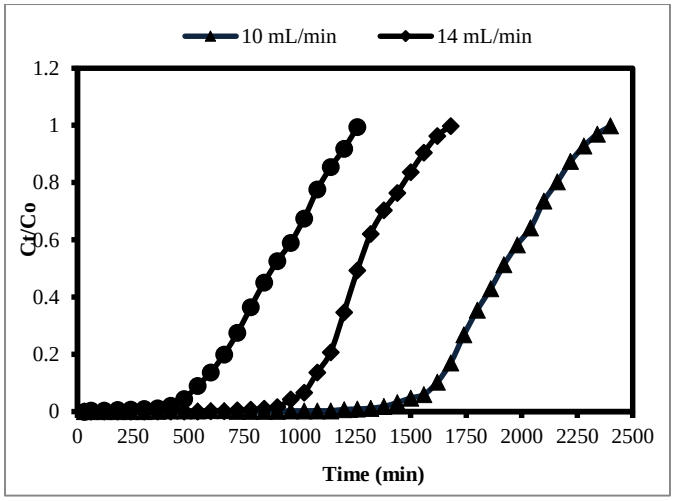

Fig 7: Effect of inlet flow rate of RO16 dye on break through curve

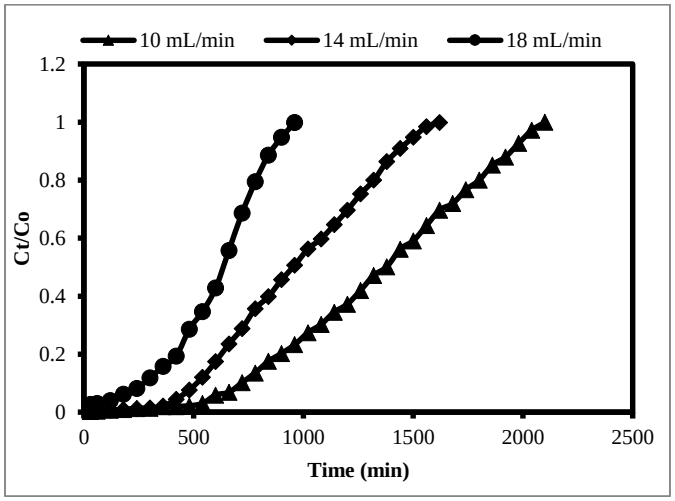

Fig 8: Effect of inlet flow rate of AR114 dye on break through curve

Effect of dye concentration on breakthrough curve

The effect of inlet dyes concentrations from 25 to 100 mg /L with the same adsorbent bed depth of 7.5 cm and solution flow rate of 14 mL/ min on the breakthrough curves is shown Figures (9 and 10). It was illustrated in Figures 7and 8 that the breakthrough time decreased with increasing inlet dyes concentration. The extension of breakthrough point in the lower dyes concentration was due to lower mass transfer in the adsorption process which resulted in the treatment of more volume of dye solution [25]. On the other hand, the exhaustion time decreased with increasing inlet dyes concentration, which can be explained that the more feeding of dyes on per unit surface area of the MKCF caused the faster saturation of the adsorbent bed [26]

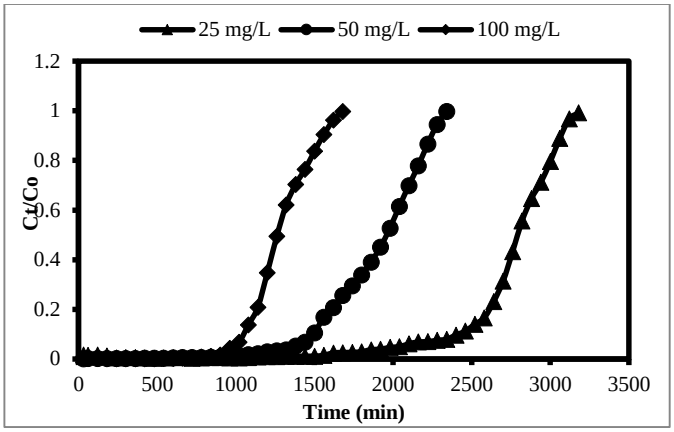

Fig 9: Effect of inlet RO16 dye concentration on break through curve

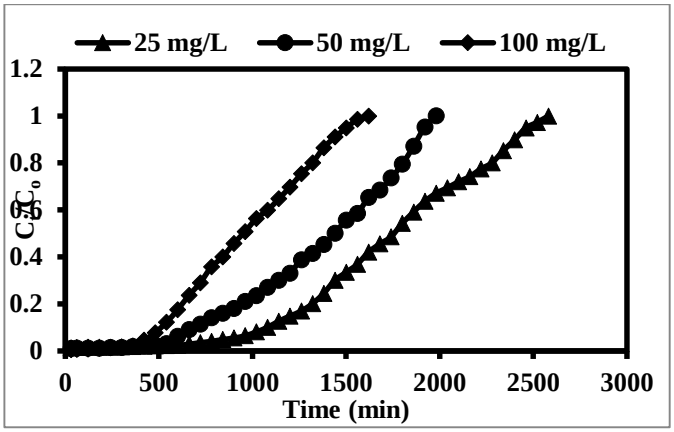

Fig 10: Effect of inlet AR114 dye concentration on break through curve

Effect of different bed depths on breakthrough curve

The breakthrough curves at different bed depths are shown in Figures (11 and 12) where it is seen that as the bed height (adsorbent mass) increases, RO16 and AR114 dyes had more time to contact with MKCF that resulted in higher removal efficiency of dyes molecules in column. So the higher bed column resulted in a decrease in the effluent dye concentration at the same service time. This was due to an increase in the surface area of adsorbent, which provided more binding sites for adsorption [27]. The slope of the breakthrough curve decreased with increasing bed height, which resulted in a broadened mass transfer zone.

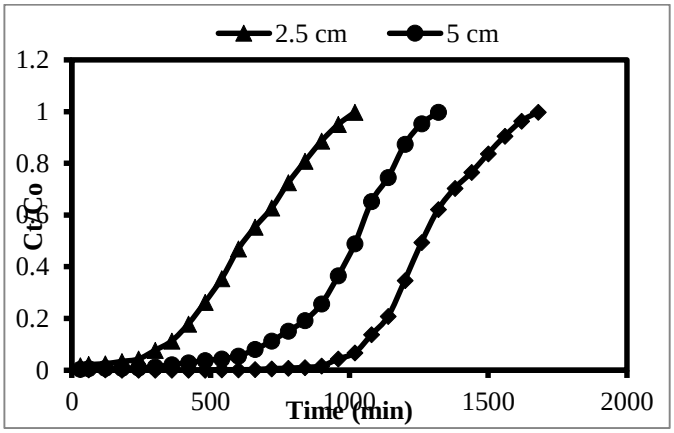

Fig 11: Effect of bed depths on break through curve for RO16 dye

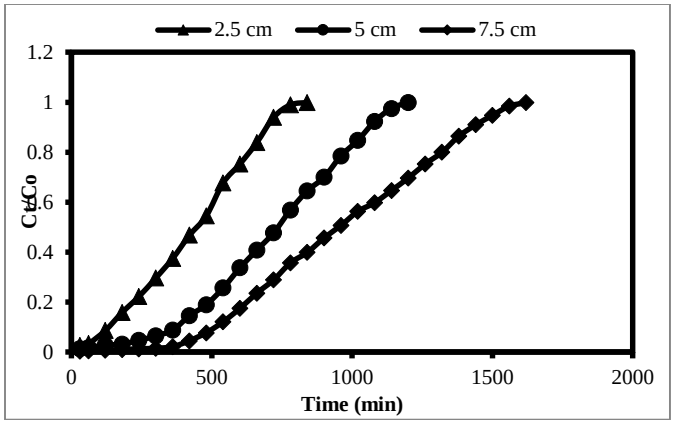

Fig 12: Effect of bed depths on break through curve for AR114 dye

Fixed bed adsorption model

Yoon–Nelson, Thomas and Adams-Bohart models are among the most significant models that are very commonly used in the design of adsorption columns. This also needs an analysis of the breakthrough curves. The effluent volume V_{eff} (mL) equation is expressed as follows:

$$V_{eff}=F*t_e \text{ (Eq. 1)}$$

By using Eq. (2), the total mass of MKCF adsorbed and qtot (mg) can be calculated. At a certain flow rate and influent concentration, q_{tot} is expressed as follows:

$$q_{tot} = \frac{F}{1000}\int_{t=t_e}^{t=0}(C_0 - C_t)\,dt \text{ (Eq. 2)}$$

By using Eq. (3), the equilibrium column capacity q_e (mg/g) can be determined.

$$q_e = q_{tot} = \frac{q_{tot}}{m} \text{ (Eq. 3)}$$

The total amount of MKCF supplied to column m_{tot} (mg) can be determined with the help of the following equation:

$$m_{tot} = \frac{F*t_e*C_O}{1000} \text{ (Eq. 4)}$$

By using Eq. (5), the removal percentage (R%) of MKCF can be determined.

$$R\% = \frac{q_{tot}}{m_{tot}} \text{ (Eq. 5)}$$

Where:

m (g) is the amount of MKCF in the fixed bed, F is the volumetric flow rate (mL/min), and C_0 and C_t (mg/L) is the influent and effluent dye concentration, respectively.

Fixed bed adsorption models

Thomas model

Thomas model parameters were determined from the linear plots of $ln\ (C_t/C_o - 1)$ versus t (min) at different initial dye concentration, bed heights and flow rates. The calculated values of maximum adsorption capacity q_e (max) and kinetic coefficient K_{TH} are summarized in Tables (4 and 5) for RO16 dye and AR114 dye respectively. It can be observed from Tables (4 and 5) that with increase concentration of dye increased, the maximum adsorption capacity increased and coefficient K_{TH} increased. This is because, with increase in concentration, the driving force for adsorption increased. The value of q_e (max) increased with increase in bed height and corresponding K_{TH} values decreased. This is because, at higher bed heights, more reactive sites were available. As the flow rate increased, the maximum adsorption capacity decreased and coefficient K_{TH} decreased. This is because the residence time of solute in the bed was less.

Table 4: Thomas model parameters for RO16 dye at different conditions using linear regression analysis

Initial RO16 dye concentration (mg/L)	Bed height (cm)	Flow rate (mL/min)	K_{TH} (mL/min mg)	q_e (mg/g)	R^2
25	7.5	14	0.084	208.978	0.7618
50	7.5	14	0.08	262.240	0.9632
100	7.5	14	0.069	355.733	0.8972
100	2.5	14	0.073	498.597	0.9916
100	5	14	0.071	399.043	0.962
100	7.5	10	0.042	389.483	0.8901
100	7.5	18	0.077	304.577	0.9627

Table 5: Thomas model parameters for AR114 dye at different conditions using linear regression analysis

Initial AR114 dye concentration (mg/L)	Bed height (cm)	Flow rate (mL/min)	K_{TH} (mL/min mg)	q_e (mg/g)	R^2
25	7.5	14	0.12	114.402	0.9764
50	7.5	14	0.072	186.574	0.9787
100	7.5	14	0.056	258.662	0.9783
100	2.5	14	0.09	330.311	0.954
100	5	14	0.064	282.565	0.986
100	7.5	10	0.04	268.095	0.986
100	7.5	18	0.07	199.837	0.9797

Yoon–Nelson model

The experimental data were fitted with Yoon-Nelson model to investigate the breakthrough characteristics of RO16 dye and AR114 dye onto MKCF. The values of k_{YN} and τ were evaluated from the linear plots of $ln\ (C_t/(C_o - C_t))$ versus t (min) at different initial dye concentration, bed heights and flow rates. The values of k_{YN} and τ are listed in Tables (6 and 7) for RO16 dye and AR114 dye respectively. The results show that with an increase in initial dye concentration and flow rate, the values of k_{YN} increased for both dyes. In addition, the time required for 50% exhaustion of column, τ (min) decreased with increase in initial dye concentration and

flow rate. This was due to the less contact time of dye solution in the column. The values of τ (min) also decreased with a decrease in bed height. At higher bed depth, more adsorption sites were available and this will increase the break through time.

Table 6: Yoon–Nelson model parameters for RO16 dye at different conditions using linear regression analysis.

Initial RO16 dye concentration (mg/L)	Bed height (cm)	Flow rate (mL/min)	K_{YN} (min^{-1})	τ (min)	R^2
25	7.5	14	0.0021	3135	0.7618
50	7.5	14	0.004	1967	0.9632
100	7.5	14	0.0069	1534	0.8974
100	2.5	14	0.0073	623	0.9916
100	5	14	0.0071	998	0.962
100	7.5	10	0.0042	2045	0.8901
100	7.5	18	0.0077	888	0.9627

Table 7: Yoon–Nelson model parameters for AR114 dye at different conditions using linear regression analysis

Initial AR114 dye concentration (mg/L)	Bed height (cm)	Flow rate (mL/min)	K_{YN} (min^{-1})	T (min)	R^2
25	7.5	14	0.003	1716	0.9764
50	7.5	14	0.0036	1399	0.9787
100	7.5	14	0.0056	970	0.9783
100	2.5	14	0.009	413	0.954
100	5	14	0.0064	707	0.986
100	7.5	10	0.004	1342	0.986
100	7.5	18	0.007	583	0.9797

Adams-Bohart model

Adams-Bohart model was applied to investigate the breakthrough behavior of RO16 dye and AR114 dye on MKCF. The values of k_{AB} and N_o were estimated from slope and intercepts of the linear graph between $ln\ (C_t/C_o)$ versus t (min) at different initial dyes concentration, bed heights, and flow rates. The model parameters are listed in Tables (8 and 9) for RO16 dye and AR114 dye respectively. From Tables (7and 8), it was observed that values of k_{AB} were found to decrease with increases in initial dye concentration and the adsorption capacity N_o increased with increase in dye concentration. The results also show that as the bed height increased, the adsorption capacity decreased for both dyes and the values of K_{AB} increased for RO16 day while decreased for AR114. In addition the adsorption capacity N_o decreased with increase in flow rate for both dyes. The values of corresponding coefficients K_{AB} increased. The decrease in adsorption capacity is because of the lower residence time of dye solution in the column.

Table 8: Adams-Bohart model parameters for RO16 dye at different conditions using linear regression analysis

Initial RO16 dye concentration (mg/L)	Bed height (cm)	Flow rate (mL/min)	K_{AB} (mL/min-mg) $*10^{-5}$	N_o (mg/L)	R^2
25	7.5	14	6.8	34795	0.8197
50	7.5	14	6	47204	0.9813
100	7.5	14	5.6	58484	0.894
100	2.5	14	4.7	97133	0.9563
100	5	14	4.9	69011	0.9941
100	7.5	10	3.5	62544	0.9168
100	7.5	18	6.1	50947	0.9019

Table 9: Adams-Bohart model parameters for AR114 dye at different conditions using linear regression analysis

Initial AR114 dye concentration (mg/L)	Bed height (cm)	Flow rate (mL/min)	K_{AB} (mL/min-mg) $*10^{-5}$	N_o (mg/L)	R^2
25	7.5	14	8	21754	0.9675
50	7.5	14	***5***.4	32395	0.9454
100	7.5	14	3.7	***48935***	0.8***874***
100	2.5	14	4.5	76018	0.8798
100	5	14	3.9	57110	0.9455
100	7.5	10	2.8	49631	0.9169
100	7.5	18	4.3	40391	0.9801

Regeneration

The feasibility of prepared sorbent depends on several factors together with the expenditure of regeneration and disposal of spent sorbent. Therefore, the anionic loaded spent adsorbent should have high regeneration efficiency for wider application in the adsorption process. The regeneration efficiency of MKCF was observed for three cycles by using 0.1 N and 0.2 N of NaOH solutions were used as an eluting

agent. The percentage removals of RO16 by using 0.1 N of NaOH on each regeneration cycles was 93%, 87% and 69% respectively. While, the percentage removals for AR114 were 94.8%, 87.5%, and 74% for each cycle respectively. On the other hand, the percentage removals of RO16 by using 0.2 N of NaOH was 93.5%, 88.7% and 72% and for AR114 was 95.74%, 89%, and 76.7% for each cycle respectively. The sorption process takes place either by physical or chemical interactions, ion exchange or combination of all types of mechanisms. By using NaOH as desorbing agents, it is dissociated releasing sufficient amounts of exchangeable OH^- ions. These take part in desorption mechanisms of anionic dyes from adsorbent surface. Overall, NaOH desorption technique was shown to be a promising way to regenerate the anionic loaded sorbent, Figures (13 and 14) shows the percentage removal of RO16 and AR114 dyes in each cycle respectively. As can be seen from results, the use of 0.2 N NaOH for regeneration process gives slightly higher percentage removals for both dyes.

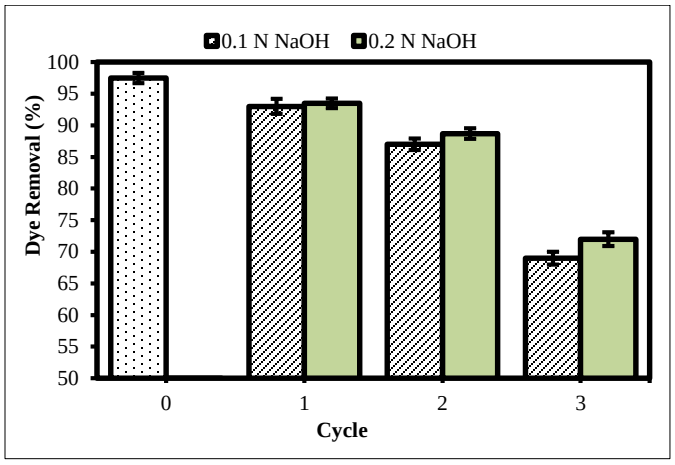

Fig 13: Adsorption cycles for RO16 on MKCF

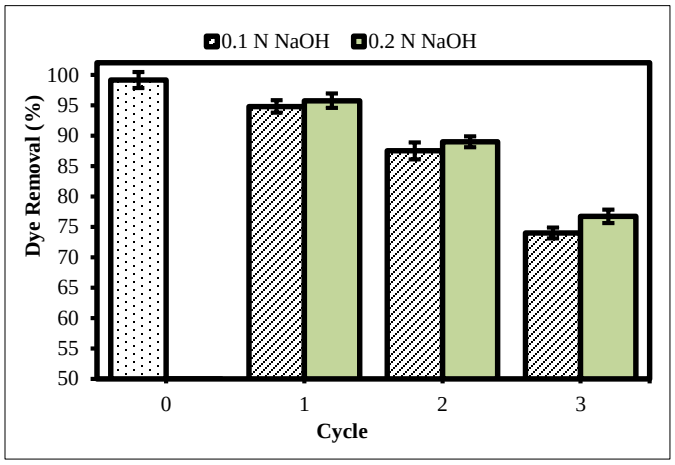

Fig 14: Adsorption cycles for AR114 on MKCF

Conclusion

In fixed bed column studies, effect of inlet flow rate, bed height and initial dye concentration on break through curve were studied. It was observed that adsorption was higher at lower flow rate, higher bed depth and lower initial dye concentration. Fixed bed column was modeled using Thomas model, Adams-Bohart model and Yoon-Nelson model. The experimental data were in good agreement with theoretical models. The study revealed that MKCF beads packed in column can be used as effective adsorbent for removal of dyes. Studies of the ability in reusing of MKCF for adsorption of RO16 and AR114 have been conducted. The column regeneration studies were carried out and the sorbent was found to be reusable with minimal decrease in its sorption capacities. This study shows that the modified kenaf core fibre was able to remove reactive and acid dyes in wastewater under specific conditions. The findings of the study indicate that MKCF has good potential in removal of dye from wastewater effluents.

References

1. Gupta VK Suhas, Tyagi I, Agarwal S, Singh R, Chaudhary M, Harit A, et al. Column operation studies for the removal of dyes and phenols using a low cost adsorbent, Global J. Environ. Sci. Manage. 2016; 2(1):1-10. Winter 2016 DOI: 10.7508/gjesm.01.001.
2. Zurhana M Hussin, Norziyanti Talib, Noraini M Hussin, Megat Hanafiah AKM, Wan Khalir KAWM. Methylene Blue Adsorption onto NaOH Modified Durian Leaf Powder: Isotherm and Kinetic Studies, American Journal of Environmental Engineering. p-ISSN: 2166-463 e-ISSN: 2166-465X, 2015; 5(3A):38-4. Doi:10.5923/c.ajee01.07, 2015.
3. Ad. Kayode A, Olugbenga SB. Dye sequestration using agricultural wastes as adsorbents, Water Resources and Industry. 2015; 12:8-24. doi:10.1016/j.wri. 09. 002, 2015.
4. Ali S, Zohreh K, Reza Al. Adsorption of cationic dye from aqueous solution onto sea shell as adsorbent low-cost, Kinetic studies, Der Pharma Chemica. 2016; 8(5):60-66,
5. Shadeera R, Nagapadma M. Modeling of Fixed Bed Column Studies for Adsorption of Azo Dye on Chitosan Impregnated with a Cationic Surfactant, International Journal of Scientific & Engineering Research. 2015; 6(2):538. ISSN 2229-5518,IJSER © 2015
6. De Ca Bruna, Ventura-Camargo, Marin-Morales MA, Azo Dyes. Characterization and Toxicity– A Review, Textiles and Light Industrial Science and Technology (TLIST), 2013, Vol. 2 Issue 2.
7. Alex S. Cleaning up one of the world's dirtiest industries will require new technology and more. 2015; 93(41):18-19. Issue Date: October 19, 2015.
8. El-Ashtoukhy E-S.Z, Mobarak AA, Fouad YO. Decolourization of Reactive Blue 19 Dye Effluents by Electrocoagulation in a Batch Recycle New Electrochemical Reactor. Int. J. Electrochem. Sci. 2016; 11:1883-1897.
9. Ka Fatemeh, Yo Habibollah, Gh Ali Asghar, He Nader Bahramifara. Thiol-incorporated activated carbon derived from Thiol-incorporated activated carbon derived from fir wood sawdust as an efficient adsorbent for the removal of mercury ion: Batch and fixed-bed column studies. j. Process Safety and Environmental Protection. 2016; 100:22-35.
10. Batmaz R, Mohammed N, Zaman M, Minhas G, Berry RM, Tam KC. Cellulose nanocrystals as promising adsorbents for the removal of cationic dyes. Cellulose, 2014; 519:21(3):1655-1665.
11. Mohammed N, Grishkewich N, Waeijen HA, Berry RM, Tam KC. Continuous flow adsorption of methylene blue

by cellulose nanocrystal-alginate hydrogel beads in fixed bed columns, Carbohydrate Polymers, 2015. http://dx.doi.org/10.1016/j.carbpol.09.099.
12. Mohandass P, Ganesan TK. Removal of Dyes Using Leaves of Morinda Pubescens as a Low Cost Green Adsorbents, International Journal of Innovative Research in Science Engineering and Technology. 2016; 5(2).
13. Khalid Mousa M, Hussein Taha A. Adsorption of Reactive Blue9 Dye onto Natural and Modified Wheat Straw a. J Chem Eng Process Technol. 2015; 6:6. http://dx.doi.org/10.4172/2157-7048.1000260.
14. Mylsamy S, Theivarasu C. Adsorption of Reactive Dye Using Low Cost Adsorbent: Cocoa (Theobroma Cacao) Shell. World Journal of Applied Environmental Chemistry. 2012; 1(1):22-29.
15. Kavitha D. Adsorptive removal of phenol by thermally modified activated carbon: Equilibrium, kinetics and thermodynamics. Journal of Environment and Biotechnology Research. 2016; 3(1):24-34.
16. Yargıç AŞ, Yarbay Şahin RZ, Özbay N, Önal E. The Effect of Different Operating Conditions on Removal of Reactive Dye by Green Carbon Adsorption, Digital Proceeding Of THE ICOEST', Cappadocia, 2013.
17. Azmier Ahmada M, Azreen Ahmad Puada N, Solomon Belloa O. Kinetic equilibrium and thermodynamic studies of synthetic dye removal using pomegranate peel activated carbon prepared by microwave-induced KOH activation, Water Resources and Industry. 2014; 6:18-35.
18. Soni M, Yadav JS, Sharma AK, Srivastava JK. Parametric optimization for adsorption of reactive orange 16 on water hyacinth root powder, Chemistry and Pharmaceutical Sciences www.ijcrcps.com, 2014; 1(6):140-147.
19. Miyaha Y, Lahrichib A, Idrissia M. Removal of cationic dye –Methylene bleu– from aqueous solution by adsorption onto corn cob powder calcined, J. Mater. Environ. Sci. 2016; 7(1):96-104. ISSN: 2028-2508.
20. Omidi Y, Kamareei B, Nourmoradi H, Basiri H, Heidari S. Hexadecyl trimethyl ammonium bromide-modified montmorillonite as a low-cost sorbent for the removal of methyl red from liquid-medium, IJE transactions A: Basics. 2016; 29(1):60-67.
21. Fa Faisal, Ib Shariff, Ha Megat Ahmad Kamal Megat. Adsorption of lead (II) onto organic acid modified rubber leaf powder: Batch and column studies, Process Safety and Environmental Protection. 2016; 100:1-8.
22. Wang L, Li. adsorption of C.I. reactive Red 228 dye from aqueous solution by modified cellulose from flax shive: kinetics, equilibrium, and thermodynamics, Ind. Crop product. 2013; 42:153-158.
23. http://www.lktn.gov.my/index.php/en/22-mengenai-lktn/piagam-pelanggan-lktn).
24. Zaini N, Khairul SNK. Adsorption of Carbon Dioxide on Monoethanolamine (MEA)–Impregnated Kenaf Core Fiber by Pressure Swing Adsorption System (PSA). Jurnal Teknologi (Sciences & Engineering). 2014; 68(5):11-16.
25. Malkoc E, Nuhoglu Y. Fixed bed studies for the sorption of chromium (VI) onto tea factory waste. Chem. Eng. Sci. 2006; 61:4363-4372.
26. Salman JM, Njoku VO, Hameed BH. Batch and fixed-bed adsorption of 2, 4-dichlorophenoxyacetic acid onto oil palm frond activated carbon. Chem. Eng. J. 2011; 174:33-40.
27. Zulfadhly Z, Mashitah MD, Bhatia S. Heavy metals removal in fixed-bed, 2001.